Processing and Application of Ceramics 13 [3] (2019) 235–243
https://doi.org/10.2298/PAC1903235A

Fabrication and characterization of nanoporous anodic alumina membrane using commercial pure aluminium to remove *Coliform* bacteria from wastewater

Hamed Aghili*, Babak Hashemi, Mohammad Ebrahim Bahrololoom, Seyed Ahamad Jenabali Jahromi

Shiraz University, School of Engineering, Department of Materials Science and Engineering, Zand Blvd., Shiraz, Iran

Received 5 November 2018; Received in revised form 9 March 2019; Accepted 15 July 2019

Abstract

Nanoporous anodic alumina (NAA) membranes were produced by anodizing process using commercially pure aluminium (1050 alloy). The optimization of processing parameters, such as applied potential, temperature and time in two different electrolyte solutions, has been performed to produce the ordered alumina nano-membrane. Nanoporous anodic alumina membrane (NAAM) was obtained by removing the aluminium substrate and opening the bottom of the pores. The microstructure of samples was studied and analysed by field emission scanning electron microscopy (FESEM). Image processing of FESEM pictures was performed with MATLAB. The results showed that at the optimum conditions of anodizing, the percentage of porosity and ordering of pores in the samples were similar to the productions of the high purity aluminium base. NAA layers that formed in sulphuric acid solution in comparison with oxalic acid had lower pore diameter (20 nm), lower inter-pore distance (45–50 nm) and higher hardness (325 HV). The optimized membranes which have been produced with the same thickness were used for separation of Coliform bacteria from the secondary clarified wastewater. The results showed that these membranes can be used as selective filters because of their desirable physical properties.

Keywords: *anodizing process, nanoporous alumina membrane, Coliform bacteria separation*

I. Introduction

Anodization is an electrochemical process that is used to produce a thick oxide layer on the surface of metals and alloys such as aluminium, titanium, and hafnium. Aluminium anodizing in sulphuric acid was reported for the first time by Gower and O'Brien in 1927 [1]. Electrolytic solutions such as sulphuric, oxalic and phosphoric acids have been used to produce nanoporous anodic alumina (NAA) [2,3]. Also, the mixture of the mentioned acids has been used [4]. An anodized layer consists of an inner dense pure oxide layer (barrier layer) and an outer porous layer. In 1973, Smith synthesized an alumina membrane by removing aluminium substrate and barrier layer from the NAA layer [5]. Masuda and Fukuda [6] synthesized self-ordered nanoporous alumina layers in 1995.

A nanoporous layer which is formed on an aluminium substrate has numerous applications in different areas such as magnetism, electronics and photonics [7–9]. Anodic alumina may also be used for the production of alumina nanowires [10]. Also, the alumina membranes have been used to fabricate biosensors, gas sensors and in tissue engineering applications, as well as for water desalination [11–15]. These membranes are also used to separate the *E-coli* bacteria from water [16].

Anodization process includes two competitive steps: i) dissolving the barrier layer at the interface between the barrier layer and the electrolyte, due to the presence of an applied electric field and ii) growth of the oxide layer at the metal-barrier layer interface. For this purpose, oxygen carrier ions formed at the interface of barrier layer-electrolyte must migrate into the barrier

* Corresponding authors: tel: +98 71 3613 3399,
e-mail: *ozlemaltintas@gmail.com, oayildirim@ktun.edu.tr*

layer at the bottom of the produced pores and metal ions should migrate from the barrier-metal interface into the barrier layer. In fact, the migration of metal and oxygen carrier ions into the barrier layer is a prerequisite for porous oxide layer's growth [17].

Barrier layer thickness and pores diameter depend on temperature and potential of the anodizing process [7,18], while the anodized layer thickness depends on the anodizing time [19]. The impurities in aluminium, which produce different expansion coefficients, influence the order and orientation of pores [20,21]. Also, initial sample preparation plays an important role in creating an appropriate structure. The electropolish process and surface roughness have a great influence on the growth of the NAA layers [22]. Additionally, the method of anodizing is very effective on the pore ordering [23]. When anodizing is done by a two-step method, the anodic oxide layer grows with highly ordered hexagonal structure [24–27]. Effective parameters which have influence on the properties of anodized layers depend on the type of electrolyte [13]. Nanoporous anodic alumina membranes (NAAM) with a certain pore diameter, interpore distance and thickness have particular importance in some specific applications. Therefore, in this study commercial pure aluminium (1050 series) was used instead of expensive high-purity aluminium and effects of different parameters such as the type of electrolyte (sulphuric acid and oxalic acid), applied potential, temperature, and method of anodizing for low cost production of an ordered nanoporous anodic alumina membrane was investigated. The optimized membranes produced with the same thickness were used for the filtration process. A secondary clarifier pool in wastewater treatment contains a variety of bacteria that are larger than 100 nm in size. The parameters were adjusted so that the thickness of the layers was identical and the diameter of the pores less than 100 nm was set. Finally, bacteria separation from secondary clarified wastewater was done by NAAMs.

II. Experimental section

Commercial pure aluminium (1050 alloy) as an anode and graphite as a cathode were used for anodization. Samples were prepared with thickness of 500 μm and radius of 2 cm. The samples were homogenized by annealing for 4 h at 500 °C and then polished by mechanical polishing. In order to degrease and remove surface contaminations, the samples were placed in an ultrasonic device containing acetone solution. Electropolishing of the samples was performed in an 85% phosphoric acid solution at 65 °C [28]. Potentials of 4, 8, 12 and 16 V and different times (1, 2 and 3 min) were employed. Then, the surface roughness of the samples was measured using a Mitutoyo machine (AD1012D, ASTM D7127). The electrolyte temperature increases during the anodization. Hence, a homemade cooling system to control electrolyte temperature was used. The real-time temperature was controlled by two thermometers inside and outside electrolyte bath. The samples were anodized under different conditions (Table 1). The permeability and mechanical properties of the membranes depend on porosity, pore diameter, and thickness. For a better comparison between the membranes synthesized in different electrolytes, NAA layers with constant thickness were produced, although the thickness of the layers depends directly on time, type of electrolyte, temperature and applied voltage. As a result, using the optimal conditions obtained in each electrolyte, the time to produce the same thickness of membranes was estimated. Thus, the anodizing time was determined in a way that layers with the same thickness were formed in the solutions of sulphuric acid and oxalic acid. In order to do this, the times of 40 and 50 min were obtained from experiments for sulphuric acid and oxalic acid, respectively. The anodized layers with the same thickness of 18 μm were achieved for both electrolytes, as a result.

Also two-step anodizing process was done on the samples by removing the primary NAA layer and again anodizing the samples with the same initial conditions. For removing the primary anodic layer, a mixture of chromic acid and phosphoric acid, with concentrations of 20 and 35 g/l, respectively, at 75 °C for 30 min was used.

In order to produce NAAM, the anodized samples were placed in solutions of copper chloride with concentrations of 0.1, 0.5 and 1 mol/l for removal of the aluminium substrate, and then placed in a 5 wt.% phosphoric acid solution at 35 °C for dissolution of the barrier layer and opening of pores.

A scanning electron microscope (FE-SEM TESCAN MIRA3 LMU) was used to investigate the morphology of the NAA layers. The chemical composition of the membranes was found through EDS analysis. Microhardness technique was used to estimate hardness of produced anodized layer. MATLAB was used for determination of surface porosity percentage of produced membranes by image processing of surface electron microscope images of membranes [29].

Optimized membranes were used to separate bacteria from water and filtering process was done. The filtered water was studied to determine the *Total Coliforms* (TC) and *Fecal Coliforms* (FC) according to the standard 9221B [30], which is related to the number of bacteria present in the water, and the efficiency of the nanomembranes to filter the bacteria was analysed.

Table 1. Components and condition of electrolytes used to produce NAA

Electrolyte type	Concentration [g/l]	Potential [V]	Temperature [°C]
H_2SO_4	1.68	15, 20, 23, 25, 26	10, 15, 20
$H_2C_2O_4$	0.3	40, 60, 80, 100, 120	0

III. Results and discussion

3.1. Electropolishing

Figure 1 shows the relationship between the surface roughness of samples and applied potential. As shown, the surface roughness changes by increasing applied potential and the electropolishing time. In the electropolishing process, there are three zones of etching, polishing and gassing [31]. Electropolishing occurs at potentials from 4 to 12 V while after that, in the gassing zone, the anode begins to dissolve and surface holes are produced. Therefore, the surface quality is reduced (Fig. 2). The most efficient electropolishing time was 2 minutes. One minute was not enough to complete electropolishing. By increasing the time, electropolishing improved. However, when electropolishing was done for 3 minutes the surface started to corrode and humps resulting from the inhomogeneous corrosion of Al substrate were formed on the surface of samples. As a result, the optimum voltage and time for electropolishing process were determined to be 12 V and 2 minutes.

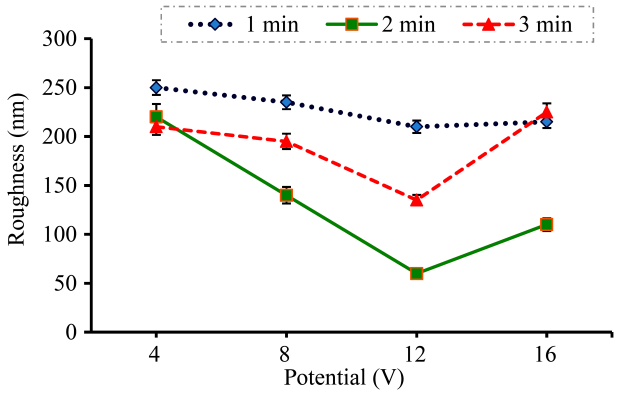

Figure 1. Effect of potential and time on the roughness of electropolished samples (roughness of as-received sample: 330 nm)

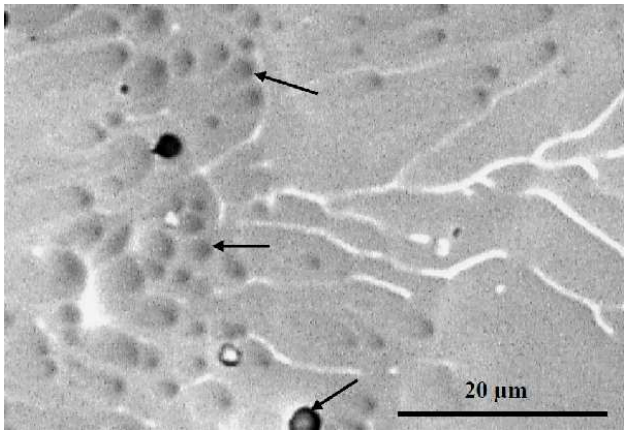

Figure 2. SEM image of holes that occur during electropolishing in the gassing zone (V = 16 V, t = 3 min)

3.2. Anodization

In order to produce ordered alumina nanoporous, the two-step anodization was carried out on the samples. Electrolyte concentration was constant for all tests and effects of other parameters, such as electrolyte type, potential and temperature, on the structure of the porous layer were investigated. In the two-step anodization process, the initial anodic layer (Fig. 3 - zone A) is dissolved by the mixture of chromic acid and phosphoric acid solution, therefore a well-prepared surface which includes suitable growth sites for ordered nanopores would be achieved (Fig. 3 - zone B). The boundary between the initial and dissolved NAA layer is illustrated in Fig. 3 - zone C.

Anodization in sulphuric acid

As shown in Table 2, anodization was done at different potentials and temperatures. At each temperature, there was a potential (burning potential) that formed micropores on the surface of the samples (Fig. 4). Burning potential was related to the temperature of the electrolyte. By increasing the electrolyte temperature, inter-

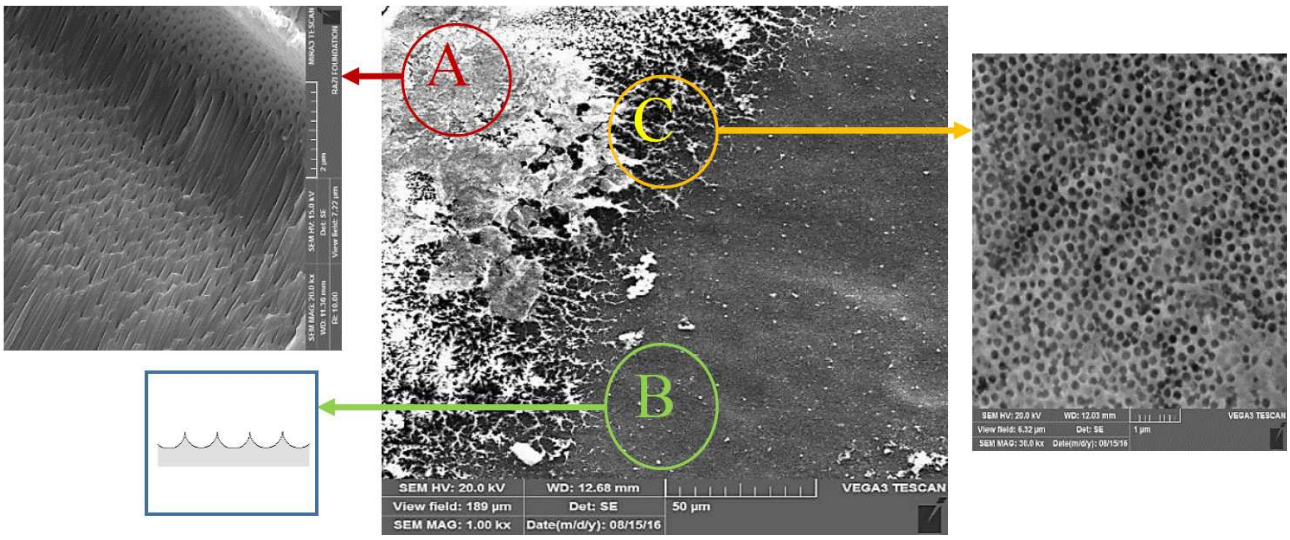

Figure 3. Dissolving NAA layer (80/O(I)/0/50), the left side shows the first anodized layer and the right side shows the surface of the sample after dissolving the anodized layer

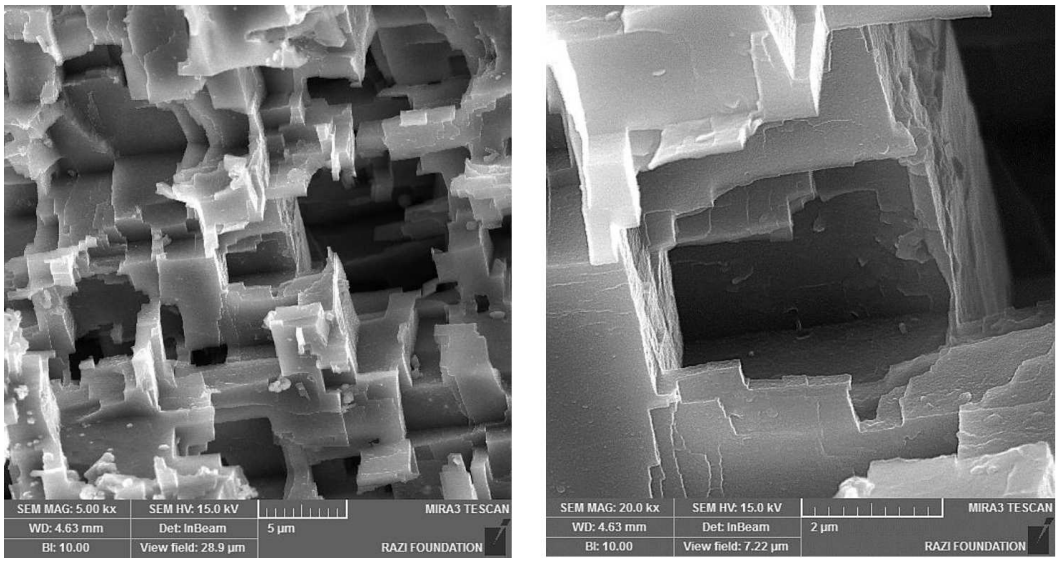

Figure 4. Surface image of micropores that were formed in sulphuric acid at 10 °C and 26 V

Table 2. Burning potential of sulphuric acid electrolyte at different temperatures

Burning potential [V]	26	25	23
Temperature [°C]	10	15	20

actions in solution were increased and the maximum applied potential was decreased. Table 2 shows the burning potential of the sulphuric acid solution according to its temperature. In order to produce a stable and uniform anodic layer, the applied voltage should be selected within the appropriate range. According to Table 2, by reducing the temperature from 20 to 10 °C, the maximum applied potential was increased.

Figure 4 shows the micropores produced on the surface of the sample by applying a potential of 26 V. The formation of micropores is similar to the mechanism of pitting corrosion [32]. As a result, to ensure stable conditions during the anodization process, 20 V potential was considered for anodizing of all samples.

Table 3 shows the results of anodizing the samples in sulphuric acid at 20 V at different temperatures and anodizing methods. As the results show, the average pore diameter and the average pore distance decrease with decreasing temperature. Therefore, an anodic porous layer structure can be formed with a high order. When the anodizing process is done in two-steps, the pore diameter size becomes more uniform and the average pore distance gets smaller. Figure 5a shows that the layer thickness was increased with increasing applied potential and temperature at constant time (40 min).

Anodization in oxalic acid

Table 3 shows the properties of porous anodized layers after anodizing in oxalic acid at different potentials. According to the results, the average pore diameter increases with increasing potential. On the other hand, the average pore distance remains almost constant from 40 to 100 V and then increases by increasing voltage to 120 V. Pore size distribution and average pore size of the samples are greater compared to those produced by anodizing in sulphuric acid. These Pores have a hexagonal shape and regularity of structure increases up to 80 V. By increasing potentials, regularity decreases and pore shape changes. Therefore 80 V can be taken as an optimum potential. With two steps anodizing and at 80 V, the average pore diameter remains relatively constant but pore size distribution becomes smaller, while pore distance decreases and pore ordering increases. Hence, the voltage of 80 V was selected as the optimal mode

Table 3. Properties of anodized samples at different anodizing conditions

Sample	Electrolyte	Potential [V]	Temperature [°C]	Time [min]	Pore diameter [nm]	Pore distance [nm]	Anodized method
20/S(I)/20/40	H_2SO_4	20	20	40	25–30	80–90	One step
20/S(I)/15/40	H_2SO_4	20	15	40	20–25	70–80	One step
20/S(I)10/40	H_2SO_4	20	10	40	17–22	55–65	One step
20/S(II)/10/40	H_2SO_4	20	10	40	20	45–50	Two step
40/O(I)/0/50	$H_2C_2O_4$	40	0	50	30–50	190–200	One step
60/O(I)/0/50	$H_2C_2O_4$	60	0	50	45–70	190–200	One step
80/O(I)/0/50	$H_2C_2O_4$	80	0	50	50–90	195–200	One step
100/O(I)/0/50	$H_2C_2O_4$	100	0	50	60–110	210–220	One step
120/O(I)/0/50	$H_2C_2O_4$	120	0	50	160–180	280–300	One step
80/O(II)/0/50	$H_2C_2O_4$	80	0	50	70–80	130–160	Two steps

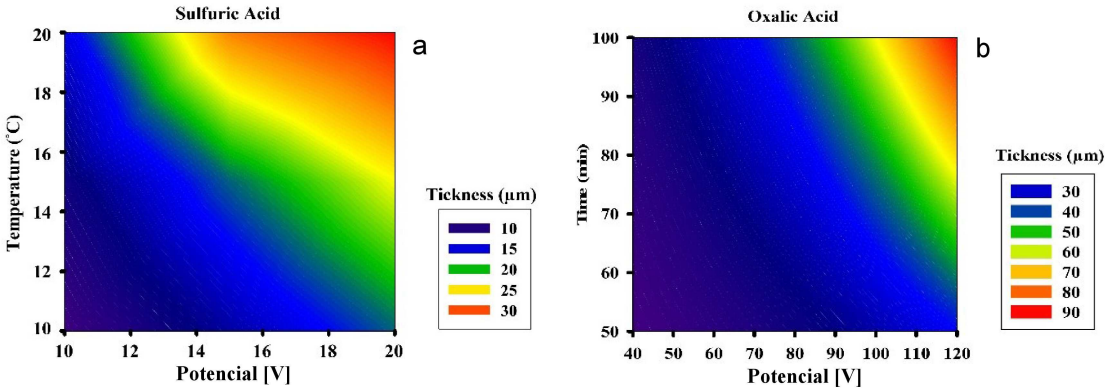

Figure 5. Plot of thickness versus potential and a) temperature (40 min) in sulphuric acid or b) time (0 °C) in oxalic acid

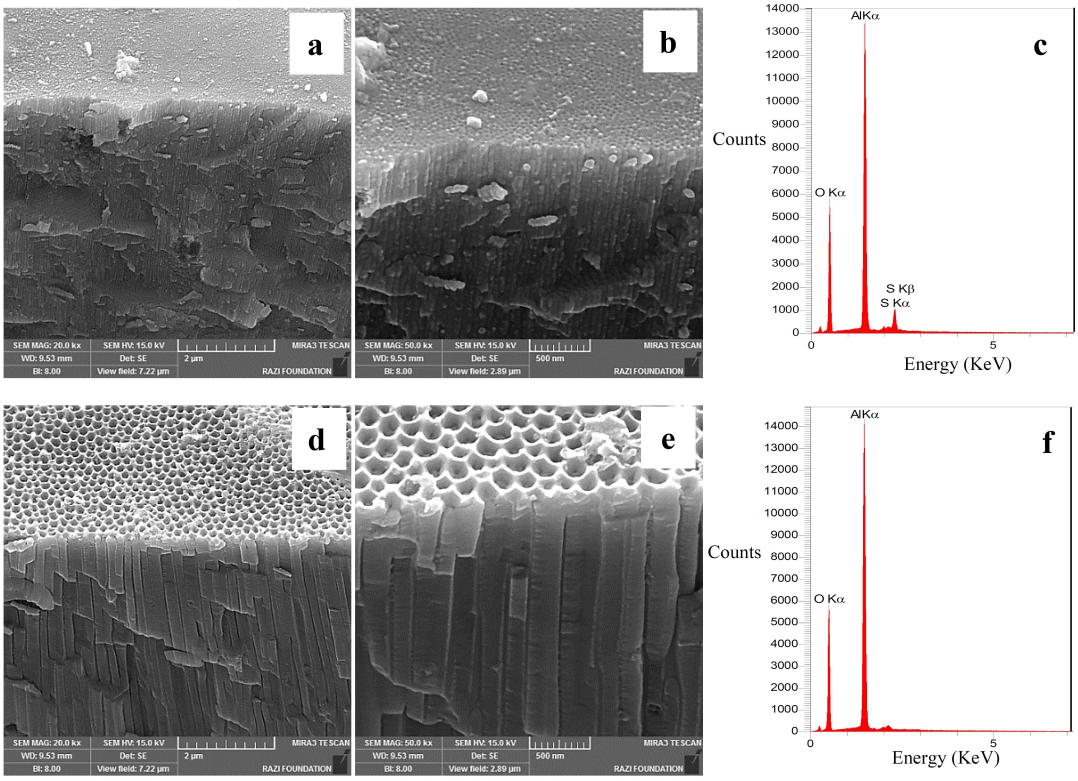

Figure 6. Microstructure of the anodized layer at optimum conditions in different magnifications and elemental analysis: (a, b and c) 20/S(II)/10/40, (d, e and f) 80/O(II)/0/50

for membrane synthesis due to the high order and suitable pore size (below 100 nm). Figure 5b shows that the layer thickness was increased with increasing applied potential and time at a constant temperature (0 °C).

3.3. Microstructure and hardness of NAA

Cross section view of anodic alumina layers synthesized at optimal conditions in both solutions is represented in Figs. 6.a,b,d,e. The pores' order is fairly acceptable and it is relatively similar to hexagonal cell structure that could be achieved for high purity aluminium anodizing. Also, elemental analysis from both layers in Figs. 6.c,f shows that aluminium and oxygen are the only elements in the anodic alumina layers. A low amount of sulphur in the layer anodized in the sulphuric acid electrolyte can be related to the presence of a number of sulphate impurities in the solution which are incorporated in the walls of the anodic film.

The pore size influences the hardness of the NAA layers and brittleness increases by decreasing pore's diam-

Table 4. Hardness of anodized layers

Sample	Electrolyte solution	Load [g]	Hardness [HV]
20/S(II)/10/40	Sulphuric acid	100	325
80/O(II)/0/50	Oxalic acid	100	269

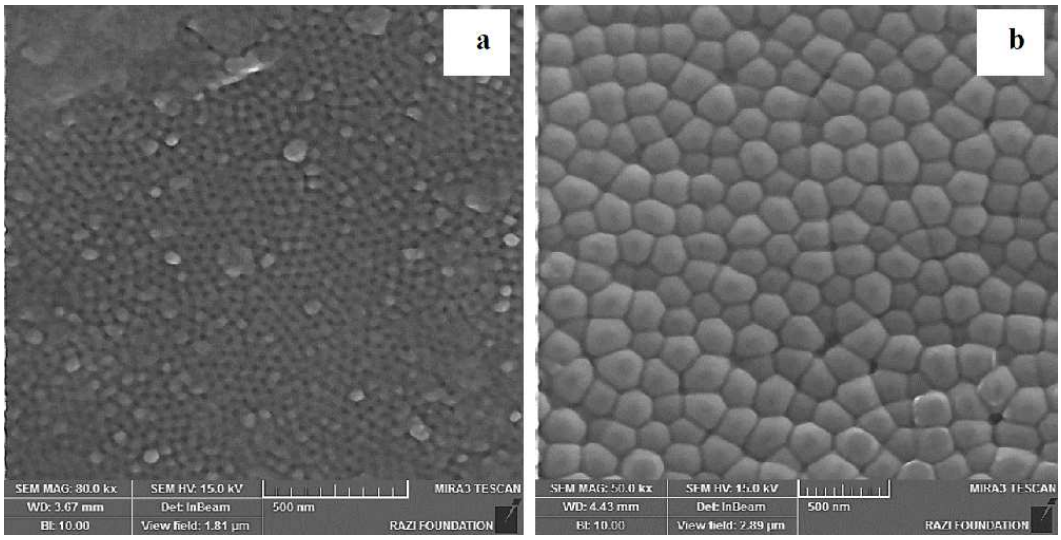

Figure 7. The bottom layer of NAA a) 20/S(II)/10/40, b) 80/O(II)/0/50

eter [33]. Table 4 shows the hardness of the anodized layers in two solutions. The produced layer in sulphuric acid has a higher hardness while being more brittle and fragile than the layer produced in oxalic acid. Because two layers have the same composition and thickness, this difference is due to the pore size and inter-pore distance.

3.4. Membrane synthesis

After production of the anodic alumina layer, with removing the aluminium and barrier layers, the porous oxide layer was converted to alumina nano-membrane. Aluminium substrate removal was done in a solution of copper chloride with different concentrations:

$$2\,Al(s) + 3\,CuCl_2(aq) \longrightarrow 3\,Cu(s) + 2\,AlCl_3(aq) \quad (1)$$

The reaction is also accompanied by the evolution of hydrogen gas:

$$2\,Al + 6\,H^+ \longrightarrow 2\,Al^{3+} + 3\,H_2 \quad (2)$$

By increasing the concentration of copper chloride, the intensity of the layer removal reactions is greatly increased and the dissolution rate of the aluminium substrate is gradually increased. Also, the rate of the reactions and the gases thus exhausted (H_2) increases. Consequently, if the pores nozzle is not closed with a protective layer during the removing process, the layer will be damaged and even leads to the failure of the anodic layer. In order to optimize the elimination time of substrates with high thickness, firstly the sample should be put in a solution with high concentration to quickly dissolve a large volume of substrates. After the thinning, the substrate will be transferred into a solution with lower concentration to continue the elimination of substrates without damaging anodic layers. Figure 7 shows the bottom layer of optimal samples in both electrolytes.

The final step for producing membrane is the elimination of the barrier layer. The barrier layer thickness depends on the applied potential and the type of electrolyte. To remove the barrier layer, a 5 wt.% solution of phosphoric acid is used at 35 °C. Phosphoric acid also causes pore widening. Thus, to avoid increasing the pore size, the appropriate time to remove the barrier layer should be selected. If the exposure time in the solution increases, the whole anodized layer will be dissolved gradually and the membrane will be completely dissolved.

3.5. Bacteria separation

The optimal samples were selected to evaluate the number of bacteria in the filtered water. The membranes produced in the sulphuric acid (20/S(II)/10/40) have failed due to the high brittleness during the filtration process, but the membranes produced in the oxalic acid (80/O(II)/0/50) showed good strength. The results of the filtration test are presented in Table 5. The amount of TC and FC in as received water was 6300 MPN per 100 ml. After the filtering process, the TC content in sample 20/S(II)/10/40 was more than 1800 MPN/ml. Due to the brittleness of the membrane and the pressure applied on the membrane surface in the filtration process, the membrane was cracked and the bacteria passed through it. The sample 80/O(II)/0/50 showed good stability to filtration and completely prevented the passing of bacteria. The TC content in this sample was less than 1.8 MPN/ml.

The pore sizes of the membranes in oxalic acid and sulphuric acid were 80 and 20 nm, respectively, which were smaller than the size of the bacteria in water (more

Table 5. Bacteriological analysis of as-received and filtered water

Sample	Total coliform [MPN/100 ml]	Fecal coliform [MPN/100 ml]
As received	6300	6300
20/S(II)/10/40	>1600	>1600
80/O(II)/0/50	<1.8	<1.8

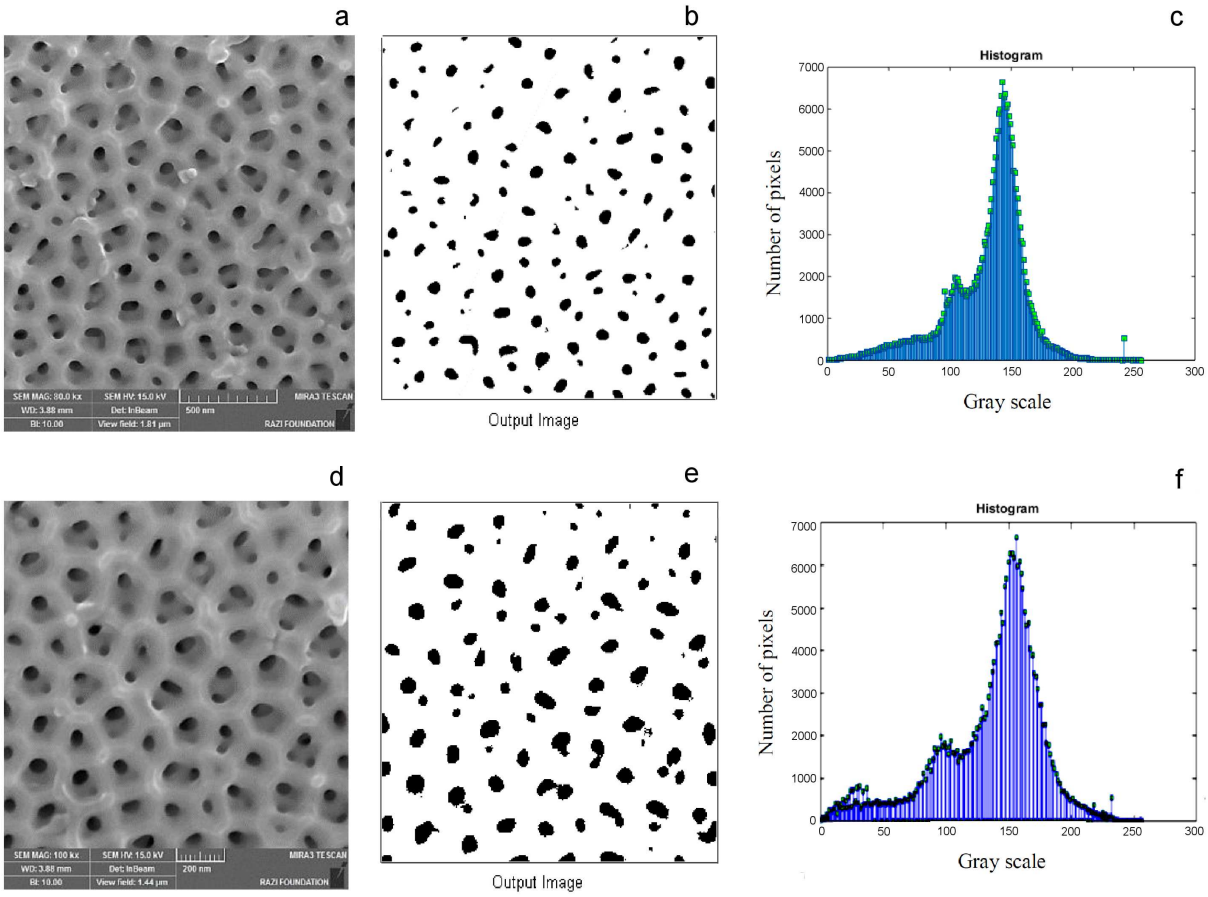

Figure 8. Image processing of the sample 80/O(II)/0/50 in two magnification: (a,d) input image, (b,e) output image and (c,f) histogram

than 100 nm). According to the obtained results, the optimal membranes produced in oxalic acid have the ability to separate bacteria in water due to the proper strength during the filtration process and the appropriate pores.

3.6. Image processing

MATLAB software was used for determination of porosity percent of porous alumina membrane (sample 80/O(II)/0/50). In the used method, each photo is defined as a 511 × 516 matrix. Each colour in the image is assigned a number in the range of 0–255 and named grayscale. In this range, 0 belongs to black and 255 to white. For image processing, a threshold consistent with the histogram of each pixel of each image is defined so that if the numerical value for each pixel is lower than the threshold, it is seen as black and otherwise it is seen as white. As a result, the image transforms into a binary form, where the pores become black and the other parts of the porous layer are white (Fig. 8). To calculate the amount of porosity of anodized layers, the ratio of black pixels number to the total pixels number was calculated. Regarding to the image processing results, the membrane porosity of the sample 80/O(II)/0/50 was obtained as 11.2% and 11.3% with magnification of 80 k and 100 k, respectively. According to the 10% porosity law, which is obtained for anodization of high purity aluminium due to the high ordering of pore structure, it is concluded that the optimal anodized layer of commercially pure aluminium in oxalic acid has pores structure relatively similar to anodized pure aluminium (hexagonal structure).

IV. Conclusions

The results of the present investigation showed that nanoporous anodic alumina membranes can be produced by anodizing commercial pure aluminium (1050 alloy) in either sulphuric acid or oxalic acid. It seems that sulphuric acid produces pores with smaller diameters (20 nm) than the pores obtained by anodizing in oxalic acid (80 nm). The inter-pore distance for the membranes prepared in oxalic acid was also found to be longer than the distance between pores produced in sulphuric acid. In order to more enhance the lattice order, we have also controlled the pores diameter and inter-pore distance via temperature and voltage changes. To fabricate membranes from anodized aluminium, it is possible to remove aluminium and barrier layer in a copper chloride solution and then phosphoric acid, respectively. These porous membranes were used as filters for removal of bacteria from water. Moreover, way, the membranes produced in oxalic acid exhibit larger pores diameter and hence less brittleness leading to more sat-

isfactory mechanical performance. The porosity content of the optimum membrane was calculated using MATLAB software.

Acknowledgement: We are sincerely grateful for helps by Dr. S.M. Arab in designing the schematic, Esmaeil Seraj in image processing and Lida Radan for her help and guidance.

References

1. P. G. Sheasby, R. Pinner, *The Surface Treatment and Finishing of Aluminum and its Alloys*, ASM International & Finishing Publications, Ohio, 2001.
2. W. Lee, R. Ji, U. Gösele, K. Nielsch, "Fast fabrication of long-range ordered porous alumina membranes by hard anodization", *Nature Mater.*, **5** [9] (2005) 741–747.
3. K. Schwirn, W. Lee, R. Hillebrand, M. Steinhart, K. Nielsch, U. Gösele, "Self-ordered anodic aluminum oxide formed by H_2SO_4 hard anodizind", *ACS Nano*, **2** [2] (2008) 302–310.
4. L. Zaraska, G. D. Sulka, J. Szeremeta, M. Jaskuła, "Porous anodic alumina formed by anodization of aluminum alloy (AA1050) and high purity aluminum", *Electrochim. Acta*, **55** [14] (2010) 4377–4386.
5. A. Smith, "Process for producing an anodic aluminum oxide membrane". *US patent US3850762*, 1974.
6. H. Masuda, K. Fukuda, "Ordered metal nanohole arrays made by a two-step replication of honeycomb structures of anodic alumina", *Science*, **268** [5612] (1995) 1466–1468.
7. H.M. Chen, C.F. Hsin, R.S. Liu, S.F. Hu, C.Y. Huang, "Controlling optical properties of aluminum oxide using electrochemical deposition", *J. Electrochem. Soc.*, **154** [6] (2007) 11–14.
8. V. Sokol, I. Vrublevsky, V. Parkun, K. Moskvichev, "Investigation of mechanical properties of anodized aluminum using dilatometric measurements", *Anal. Bioanal. Chem.*, **375** [7] (2003) 968–973.
9. S. Kawai, M. Yamamuro, "Interference coloring of dual-anodized films on aluminum containing electrolytically deposited thin metal layers", *Plat. Surf. Finish.*, **84** [5] (1997) 116–119.
10. M. Sadeghpour-Motlagh, K. Mokhtari-Zonouzi, H. Aghajani, M.G. Kakroudi, "Effects of etching time and NaOH concentration on the production of alumina nanowires using porous anodic alumina template", *J. Mater. Eng. Perform.*, **23** [6] (2014) 2007–2014.
11. A. Santos, T. Kumeria, D. Lusic, "Nanoporous anodic alumina: a versatile platform for optical biosensors", *Materials*, **7** (2004) 4297–4320.
12. H. Lira, R. Paterson, "New and modified anodic alumina membranes: preparation and characterization by gas diffusion of 5 nm pore size anodic alumina", *Membrane. Sci.*, **206** (2002) 375–387.
13. G. Poinern, A. Nurshahidah, D. Fawcett, "Progress in nano-engineered anodic aluminum oxide membrane development", *Materials*, **4** [3] (2011) 487–526.
14. C. Lai, C. Cheng, Y. Huang, W. Chang, F. Tseng, Y. Chueh, "Desalination of saline water by nanochannel array through manipulation of electrical double layer", *Nano Energy*, **12** (2015) 394–400.
15. D. Bruggemann, "Nanoporous aluminum oxide membranes as cell interfaces", *J. Nanomaterials*, **2013** (2013) 460870.
16. A.M. Zimer, M.P. Machado, L.J. Dalla Costa, P.T.L. Ike, M.R.C. Lemma, C.F. Yamamoto, C.F. Ferreira, D.H.F. Souza, C.R. De Olivieira, E.C. Pereira, "Optimized porous anodic alumina membranes for water ultrafiltration of pathogenic bacteria E. coli", *J. Nano Sci. Nano Tech.*, **16** [6] (2016) 6526–6534.
17. A. Eftekhari, *Nanostructured Materials in Electrochemistry*, John Wiley & Sons, 2008.
18. T. Aerts, Th. Dimogerontaki, I. De Graeve, J. Fransaer, H. Terryn, "Influence of the anodizing temperature on the porosity and the mechanical properties of the porous anodic film", *Surf. Coat. Technol.*, **201** [16] (2007) 7310–7317.
19. I. Tsangaraki-Kaplanoglou, S. Theohari, Th. Dimogerontakis, Y.M. Wang, H. Kuo, S. Kia, "Effect of alloy types on the anodizing process of aluminum", *Surf. Coat. Technol.*, **200** [8] (2006) 2634–2641.
20. J. Choi, *Fabrication of monodomain porous alumina using nanoimprint lithography and its applications*, Martin Luther Universitiat Halle Wittenberg, 2004.
21. D. Lo, R.A. Budiman, "Fabrication and characterization of porous anodic alumina films from impure aluminum foils", *J. Electrochem. Soc.*, **154** [1] (2007) 60–66.
22. L.F. Mendes, A.S. Moraes, J.S. Santos, F.L. Leite, F. Trivinho-strixino, "Investigation of roughness and specular quality of commercial aluminum (6061 alloy) for fabrication of nanoporous anodic alumina films", *Surf. Coat. Technol.*, **310** (2017) 199–206.
23. J.M. Montero-Moreno, M. Sarret, C. Müller, "Self-ordered porous alumina by two step anodizing at constant current: Behavior and evolution of the structure", *Micropor. Mesopor. Mat.*, **136** [1-3] (2010) 68–74.
24. M.H. Lee, N. Lim, D.J. Ruebusch, A. Jamshidi, R. Kapadia, R. Lee, T.J. Seok, K. Takei, K.Y. Cho, Z. Fan, H. Jang, M. Wu, G. Cho, A. Javey, "Roll-to-roll anodization and etching of aluminum foils for high-throughput surface nanotexturing", *Nano Lett.*, **11** [8] (2011) 3425–3430.
25. A. Santos, L. Vojkuvka, J. Pallares, "Cobalt and nickel nanopillars on aluminium substrates by direct current electrodeposition process", *Nanoscale Res. Lett.*, **4** [9] (2009) 1021–1028.
26. W.J. Stepniowski, A. Nowak-Stepniowska, M. Michalska-Domanska, M. Norek, T. Czujko, Z. Bojar, "Fabrication and geometric characterization of highly-ordered hexagonally arranged arrays of nanoporous anodic alumina", *Polish. J. Chem. Techol.*, **16** [1] (2013) 63–69.
27. E. Moyen, L. Santinacci, L. Masson, W. Wulfhekel, M. Hanbucken, "A novel self-ordered sub-10 nm nanopore template for nanotechnology", *Adv. Mater.*, **24** [37] (2012) 5094–5098.
28. P. Neufeld, D.M. Southall, "The electropolishing of aluminium", *Electrodep. Surf. Treat.*, **3** [3] (1975) 159–168.
29. *MATLAB and Statistics Toolbox Release 2015b*, The MathWorks, Inc., Natick, Massachusetts, United States
30. A.D. Eaton, L.S. Clesceri, A.E. Greenberg, M.A.H. Franson, *Standard methods for the examination of water and wastewater*, American Water Works Association & Water Environment Federation, Washington, DC: American Public Health Association, 1998.
31. H. Adelkhani, S. Nasoodi, A.H. Jafari, "A study of the morphology and optical properties of electropolished aluminum in the Vis-IR region", *Int. J. Electrochem. Sci.*, **4** [2] (2009) 238–246.

32. G.Q. Ding, R. Yang, J.N. Ding, N.Y. Yuan, W.Z. Shen, "Microscale steps and micro-nano combined structures by anodizing aluminum", *Appl. Surf. Sci.*, **256** [21] (2010) 6279–6283.

33. P. Ramana Reddy, K.M. Ajith, N.K. Udayashankar, "Micro and nanoindentation analysis of porous anodic alumina prepared in oxalic and sulphuric acid", *Ceram. Int.*, **42** [15] (2016) 17806–17813.